Article

Bionic Thermoelectric Response with Nanochannels

Kexin Chen, Lina Yao, and Bin Su

J. Am. Chem. Soc., **Just Accepted Manuscript** • DOI: 10.1021/jacs.9b03569 • Publication Date (Web): 08 May 2019

Bionic Thermoelectric Response with Nanochannels

Kexin Chen, Lina Yao and Bin Su*

Institute of Analytical Chemistry, Department of Chemistry, Zhejiang University, Hangzhou 310058, China

KEYWORDS thermoelectric response, temperature change, diffusion potential, permselectivity, silica nanochannels

ABSTRACT: Thermosensation, the ability to detect the environmental temperature change, is one of most ancient and crucial processes for the survival of all living organisms. Mammals use temperature-sensitive transient receptor potential (thermoTRP) cation channels as thermometers to convert the temperature change into electrical signals that are finally received as action potentials by nerve endings. In this work we report the bionic thermosensation by solid-state hybrid nanochannels based on the principle of thermally sensitive permselective ion transport. The hybrid nanochannels possess an asymmetric structure, consisting of ultrasmall silica nanochannels (~2.3 nm in diameter, ~100 nm in length) supported by large-sized track-etched poly(ethylene terephalate) conical nanochannels. When the hybrid nanochannels are engineered to separate two electrolyte solutions, the temperature change in one solution can be directly converted into trans-nanochannel diffusion potential, akin to the natural thermosensation process. Two bionic modes, namely in the absence and presence of a concentration gradient, were studied to imitate the natural thermosensation of thermoTRP ion channels and shark, respectively. In both cases, real-time thermoelectric response was captured with a fast relative response speed (electrical response time vs. temperature change time) of higher than 98%, as well as excellent stability and reversibility. Moreover, the nanochannels are highly sensitive to the thermal stimulus, showing a sensitivity of 0.7 mV/K comparable to the natural thermosensation. The experimental results coincide well with the theoretical relationship between electrical response and temperature change derived in terms of a quasi-steady-state ion transport model. Finite element simulations based on coupled Poisson-Nernst-Plank (PNP) and Einstein-Stokes equations were also performed, confirming that the sensitive thermoelectric response originates from the highly cationic selectivity of nanochannels.

INTRODUCTION

The organism genome encodes hundreds of ion channels with divergent structures and functions.[1] These ion channels present fast and selective responses to different chemical and physical stimuli, which have triggered extensive research on bio-inspired nanochannel fabrication and natural behaviour imitation.[2,3] Among various stimulus-responsive functions, thermosensation, the ability to sense the environmental temperature to avoid noxious heat or cold, is crucial for the survival of all living organisms. In recent years, various types of biological ion channels, such as thermosensitive transient receptor potential (thermoTRP) cation channels, have been identified as highly sensitive molecular thermometers. ThermoTRP ion channels can convert thermal stimuli into electrical signals, which then convey from the periphery to central nervous system in the form of action potentials.[4-6]

Although various bionic structures consisting of nanopore or nanochannel, under the inspiration of examples from nature, responsive to molecules,[7] pH,[8] light,[9] and ions[10] have been reported, those temperature-sensitive remains less unexplored and has not been fully developed yet. In early studies, Spohr et al. explored the use of poly-*N*-isopropylacrylamide (polyNIPAM) hydrogel to chemically graft solid-state channels in ion track membranes to control the molecular transport by temperature change.[11] In 2006, Movileanu and co-workers used temperature-responsive elastin-like polypeptide loops to engineer the protein pores, which then functioned as thermally sensitive gate to control the ion flow.[12] In the similar way, the Azzaroni group employed nanochannels modified with thermally responsive polyNIPAM brushes as molecular gates actuated by temperature-driven conformational transitions.[13] Jiang et al. also designed smart nanochannels by grafting temperature-sensitive molecular brushes onto walls or entrances of channels for gated or rectified transport.[14-16] However, the responses to temperature change achieved in these models rely on in most cases extrinsic temperature-sensitive gatekeepers. Moreover, the responses are usually measured as the current flow,[17] instead of potential in nature behaviours. To the best of our knowledge, the thermosensation arising from the intrinsic structure of nanochannels have not been observed yet in the form of potential.

In this work, a highly cationic selective hybrid nanochannel membrane was fabricated, which possessed an asymmetric structure consisting of ultrasmall silica isoporous nanochannels (designated as SIM, ~2.3 nm in diameter, ~100 nm in length) and large-sized track-etched poly(ethylene terephalate) (PET) conical nanochannels. Thus prepared membrane with flow-through nanochannels, designated as SIM/PET hybrid nanochannels, was engineered to separate two electrolyte solutions to study the thermoelectric response to temperature change. Two bionic modes, in the absence and presence of a concen-

tration gradient, were studied to imitate the natural thermosensation of thermoTRP ion channels and shark, respectively. Due to ultrasmall size and negatively charged surface, the hybrid nanochannels are highly permselective, screening the transport of anions while favouring that of cations, thus resulting in detectable trans-nanochannel diffusion potential difference, which was recorded under the open-circuit condition as the measure of thermoelectric response. A tiny temperature gradient across hybrid nanochannels can induce a very sensitive thermoelectric response, with a sensitivity of 0.7 mV K^{-1} comparable to nature thermosensation systems. Moreover, the hybrid nanochannels can respond very fast to the temperature change with a relative response speed (response time vs. temperature change time) of higher than 98%. In addition, the thermoelectric response is also stable, reproducible and reversible. Theoretical derivation based on the quasi-steady-state ion transport model, and finite element simulations based on coupled Poisson-Nernst-Plank (PNP) and Einstein-Stokes equations, were performed to rationalize the origin of thermoelectric response of hybrid nanochannels, showing that the highly cationic selectivity is a crucial factor to achieve a large electrical signal in response to thermal stimulus.

THEORETICAL CONSIDERATION

Here a simplified model, as illustrated in **Figure 1a**, is employed to derive the thermoelectric response of nanochannels. Two solutions, designated as α and β, respectively, containing 1:1 electrolyte (KCl or NaCl) at a concentration of c^{α} and c^{β}, are separated by nanochannels. In this work, KCl or NaCl was used as the electrolyte. Accordingly, the temperature of two solutions is T^{α} and T^{β}. Considering a quasi-steady state for irreversible ion transport through nanochannels from one solution to another, we have the following equation,

$$t_{+}\left(\overline{\mu}_{+}^{\beta}-\overline{\mu}_{+}^{\alpha}\right)+t_{-}\left(\overline{\mu}_{-}^{\alpha}-\overline{\mu}_{-}^{\beta}\right)=0 \qquad (1)$$

where t_i and $\overline{\mu}_i$ (i = +, –, refer to cation and anion, namely K^+/Na^+ and Cl^- in this work) are the transference number and electrochemical potential of ions, respectively.

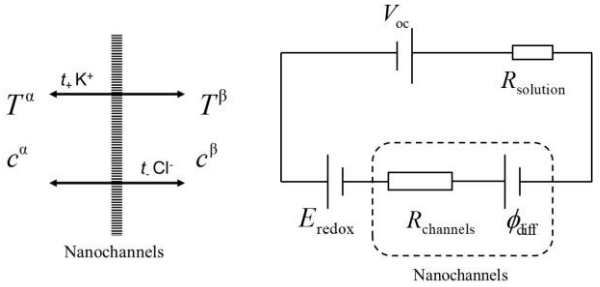

Figure 1. (a) The simplified model of ion transport across nanochannels in the present of temperature gradient. (b) The equivalent circuit of experimental measurement of thermoelectric response under the open-circuit condition.

For simplicity, both the activity coefficient and the standard electrochemical potential of ions are assumed to be uniform and do not vary with temperature change. It is reasonable because in this work only a small temperature change ($\Delta T \leq 10$ K) was used as the stimulus. Their contributions to the trans-nanochannel potential are indeed very small.[17,18] According to **eq. 1**, the trans-nanochannel diffusion potential (ϕ_{diff}) in response to the temperature change can be derived as (see the supporting information file for more details, Section S1),

$$\phi_{diff}=\left(\phi^{\alpha}-\phi^{\beta}\right)=\left(2t_{+}-1\right)\left(\frac{RT^{\beta}}{F}\ln c^{\beta}-\frac{RT^{\alpha}}{F}\ln c^{\alpha}\right) \qquad (2)$$

According to **eq. 2**, ϕ_{diff} is a function of both solution temperature and ion concentration.

From the experimental viewpoint, what can be measured usually is the open-circuit potential (V_{oc}), e.g., by two silver/silver chloride (Ag/AgCl) reference electrodes immersed in solutions, as done in this work. **Figure 1b** shows the equivalent circuit of such a system, in which V_{oc} represents the sum of ϕ_{diff} (the direction from α to β is defined to be positive in this work), the difference of redox potentials of two Ag/AgCl electrodes (E_{redox}) and the ohmic potential drop across nanochannels and electrolyte solution ($iR_{channel}$ and $iR_{solution}$, i denotes the ionic current). Because V_{oc} was measured under the open-circuit condition where the system was put in series with a very high input resistance. Therefore, i is nearly zero in the circuit and we can reasonably neglect the ohmic potential drop. In this case, V_{oc} is given by (see the supporting information for more details, Section S1),

$$V_{oc}=-2t_{+}\left(\frac{RT^{\beta}}{F}\ln c^{\beta}-\frac{RT^{\alpha}}{F}\ln c^{\alpha}\right) \qquad (3)$$

We studied the thermoelectric response of two model systems, namely in the absence and presence of concentration gradient across nanochannels, to imitate the thermosensation of thermoTRP ion channels and shark, respectively. In the first case (namely $c^{\alpha} = c^{\beta} = c$), the variations of ϕ_{diff} and V_{oc} with the temperature change are expressed as,

$$\Delta\phi_{diff}\left(T\right)=\left(2t_{+}-1\right)\frac{R}{F}\Delta T\ln c \qquad (4)$$

$$\Delta V_{oc}\left(T\right)=-2t_{+}\frac{R}{F}\Delta T\ln c \qquad (5)$$

where ΔT ($\Delta T = T^{\beta} - T^{\alpha}$) is the magnitude of temperature change, namely the instantaneous temperature difference between two solutions separated by nanochannels. In the second case (namely $c^{\alpha} \neq c^{\beta}$), they are given by,

$$\Delta\phi_{diff}\left(c,\,T\right)=\left(2t_{+}-1\right)\frac{R}{F}\Delta T\ln c^{\mathrm{T}} \qquad (6)$$

$$\Delta V_{oc}\left(c,\,T\right)=-2t_{+}\frac{R}{F}\Delta T\ln c^{\mathrm{T}} \qquad (7)$$

where c^{T} is the electrolyte concentration in the solution where its temperature is changed.

Eqs. 4-7 have two apparent indications, one of which is the linear dependence of both $\Delta\phi_{diff}$ and ΔV_{oc} on ΔT. The second is that the sensitivity of thermoelectric response depends heavily on t_+. That is to say, the permselectivity of nanochannels is a decisive parameter for the generation of a large ϕ_{diff} in order to achieve a sensitive response to temperature change.

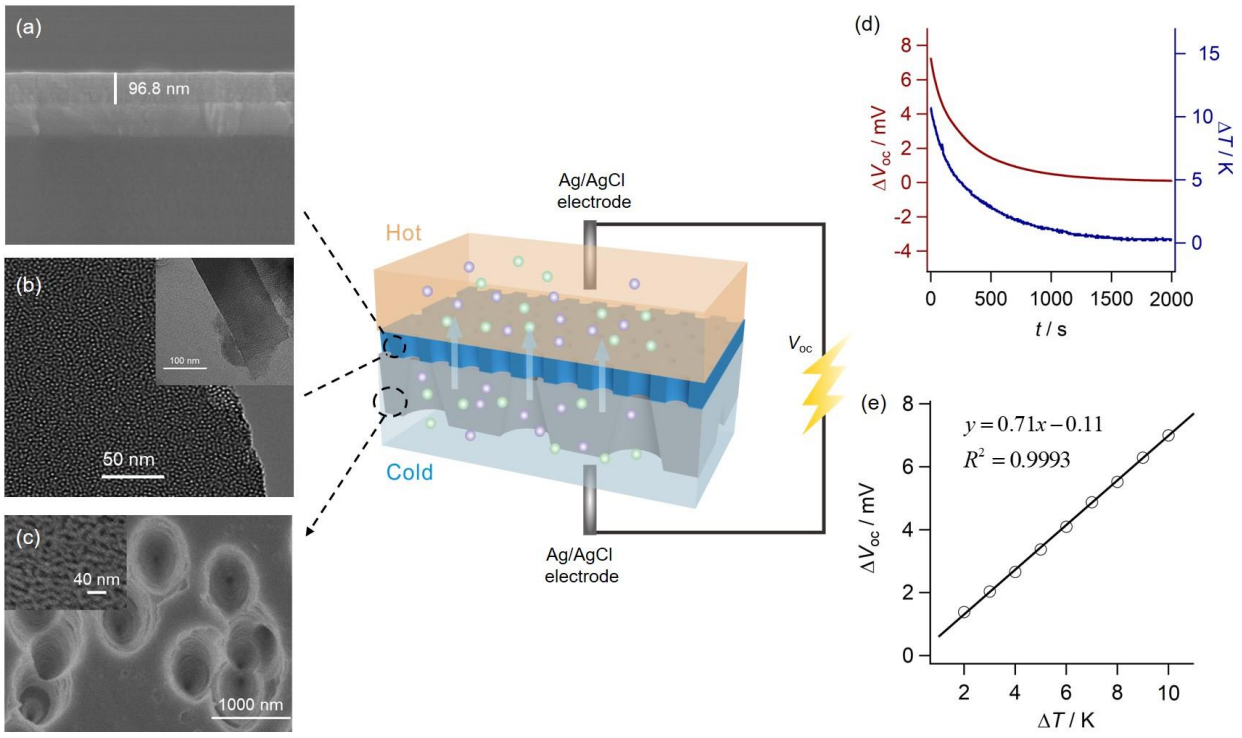

Figure 2. (a) The cross-section view of SEM image showing the thickness of SIM grown on ITO. (b) The top-view TEM image of SIM showing a high density of nanochannels. The inset is high-resolution TEM image of cross-section of SIM. (c) SEM image of the base face of PET membrane with conical nanochannels. The inset is that of the tip face. (d) Thermoelectric responses of hybrid nanochannels squeezed in between two solutions containing 10 mM KCl (pH = 5.9). The synchronous time evolution of ΔV_{oc} (red curve) and ΔT (blue curve) is displayed. (e) The dependence of ΔV_{oc} on ΔT for the thermoelectric response of hybrid nanochannels. The solid lines represent the linear fitting curves. The graph in the middle schematically illustrates the structure of SIM/PET hybrid nanochannels and experimental configuration for the measurement of V_{oc}.

RESULTS AND DISCUSSION

Fabrication of SIM/PET Hybrid Nanochannels. More experimental details on the preparation of SIM, PET with conical nanochannels and SIM/PET hybrid nanochannels can be found in the supporting information (see Section S2 and **Figure S1**). The SIM layer was primarily grown on the surface of indium tin oxide (ITO) glass using the Stöber solution growth approach.[19] The thickness of SIM is ca. 96.8 nm, as seen from the cross-section scanning electron microscope (SEM) image (see **Figure 2a**). From the top-view transmission electron microscope (TEM) image shown in **Figure 2b**, a high density of pores (roughly 16.7%) appeared as bright dots with a uniform pore size (ca. 2.3 nm in diameter) can be identified. The high resolution cross-section TEM image in the inset of **Figure 2b** shows aligned nanochannels and also confirms a thickness of ca. 100 nm. **Figure 2c** and its inset display SEM images of two surfaces of track-etched PET membrane, showing large-sized pores of 750-900 nm in diameter on one side and small ones of 10-15 nm in diameter on the opposite side. These two sides are designated as the base and tip faces, respectively. The latter was employed to adhere with SIM to prepare SIM/PET hybrid nanochannel membrane, using the approach reported previously.[20-22]

Since the first observation in a conical glass nanopipette,[23] ion current rectification (ICR) has been extensively investigated for its widespread potential applications. ICR is usually observed for nanochannels with asymmetric factors, including structure, charge or concentration asymmetry. Moreover, the magnitude of ICR depends on the degree of asymmetry, the surface charge density on nanochannel surface and the thickness of electric double layer (EDL) comparable to channel size. **Figure S2** compares the current-voltage (*I-V*) characteristic of PET conical nanochannels and SIM/PET hybrid nanochannels in 10 mM KCl. Apparently, an enhanced ionic current rectification was observed, with the rectification ratio ($|I_{+1.0\,V}/I_{-1.0\,V}|$) increasing from 3.6 to 9.1, confirming the successful preparation of layered nanochannel structure. The high pore density, ultra-small thickness and high surface charge density (due to Si-OH deprotonation) of silica nanochannels are responsible of a better ion-selectivity of hybrid structure. Moreover, the ionic current did not decrease drastically (from 24.5 nA to 16.5 nA at +1.0 V) after SIM was adhered to PET nanochannels, indicating that silica nanochannels have a negligible effect on the ion permeability thanks to its high pore density.

Bionic Thermoelectric Response without Concentration Gradient. All living organisms, from bacteria to plants and animals, have the ability to sense change in the environmental temperature and to provoke subsequent thermoregulatory actions. This fundamental process, called as peripheral thermosensation, is absolutely crucial for survival of organisms. In recent years, it has been identified that mammals use ion channels, such as types of thermoTRP cation channels, as highly sensitive molecular thermometers to transduce the temperature change into electrical signals, which finally perceived as action potentials by nerve endings. As shown in **Figure S2**, the SIM/PET hybrid nanochannels display a high selectivity towards cations. In terms of **eqs. 4-7**, highly permselective membranes are promising to imitate the thermosensation function of thermoTRP ion channels.

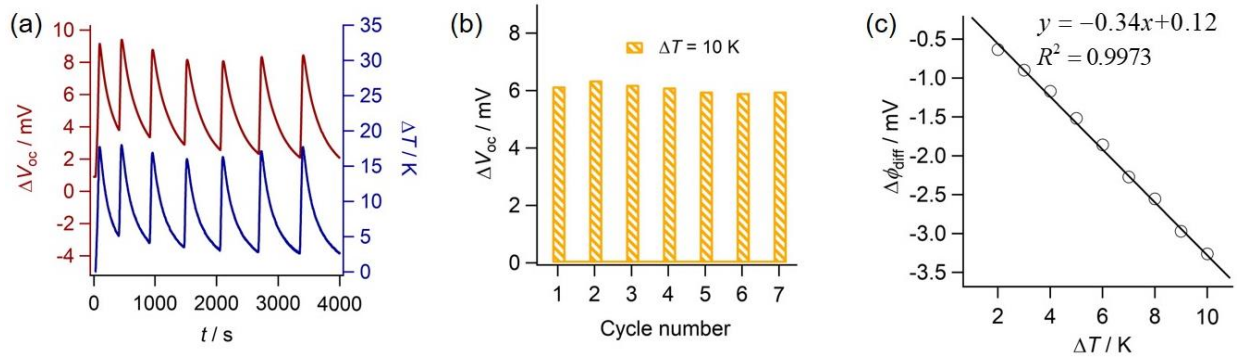

Figure 3. (a) Continuous and synchronous time evolution curves of ΔV_{oc} (red) and ΔT (blue) recorded with SIM/PET hybrid nanochannels in 10 mM KCl for seven temperature variation cycles. (b) The stability and reproducibility of ΔV_{oc} in response to ΔT = 10 K for seven cycles. (c) The dependence of $\Delta\phi_{diff}$ on ΔT. $\Delta\phi_{diff}$ values were estimated by subtraction of E_{redox} from ΔV_{oc}. The solid line corresponds to a linear fitting to **eq. 4**.

To study thermoelectric response of SIM/PET hybrid nanochannels, a home-made experimental setup was engineered for synchronous measurement of T and V_{oc}. The nanochannels were mechanically fixed by a cell to separate two aqueous solutions. The one contacted with SIM was warmed up by a digitally controlled ceramic micro-heater, while that on the other side not. The instantaneous temperature of two solutions, designated as $T_{b\text{-}SIM}$ and $T_{b\text{-}PET}$, were recorded by two immersed micro-thermometers, and meanwhile V_{oc} was measured by two Ag/AgCl electrodes. We here analyze the temperature difference between two solutions (namely $\Delta T = T_{b\text{-}SIM} - T_{b\text{-}PET}$) and the change of V_{oc} relative to the initial value (namely ΔV_{oc}).

Shown in **Figure 2d** are synchronous time evolution curves of ΔT and ΔV_{oc} recorded with SIM/PET hybrid nanochannels. In order to imitate biological systems, ΔT was limited to a range less than 10 K. It is obvious that, once the heating was stopped, both ΔV_{oc} and ΔT synchronously decreased with time slowly. It should be noted that, in agreement with the theoretical derivation by **eq. 5**, ΔV_{oc} was independent on the initial temperature but only ΔT. The variation of ΔV_{oc} with ΔT is further plotted in **Figure 2e**, showing a linear dependence coincident with **eq. 5**. The slope of linear fitting lines expresses the sensitivity of thermosensation, which is 0.70 mV K^{-1} for SIM/PET hybrid nanochannels. The thermoelectric response of PET conical nanochannels was also measured and compared, as displayed in **Figure S3a**. Although a linear dependence of ΔV_{oc} on ΔT was also observed, a small slope gave a low thermosensation sensitivity of 0.44 mV/K. It is clear that the thermal sensitivity of SIM/PET hybrid nanochannels is 1.6 times higher than that of PET conical nanochannels, because of higher cationic selectivity of the former, arising from much smaller channel size and higher surface charge density of silica nanochannels. Indeed, from the slope of linear lines shown in **Figures 2e** and **S3b**, t_+ (for K^+ in this case) can be calculated to be 0.90 for SIM/PET hybrid nanochannels and 0.55 for PET conical nanochannels, respectively. We would like to emphasize that the thermal sensitivity of SIM/PET hybrid nanochannels (namely a value of ΔV_{oc} as big as 0.70 mV in response to ΔT = 1 K) is high enough to function as a thermoelectric signal converter or a sensitive thermometer. In order to further prove that the sensitivity arises from the cationic permselectivity, the similar measurements were performed with KCl solution at pH = 3.0. As displayed in **Figure S4**, the sensitivity of thermoelectric response and t_+ were 0.52 mV K^{-1} and 0.66. The decrease was caused by the decrease of surface charge density due to protonation of surface carboxylic groups on PET and protonation of silanol groups on silica.

Apart from high sensitivity, a rapid response to temperature change is also very important, because it may have important and even harmful effects on organisms. Therefore, we studied the response speed of SIM/PET hybrid nanochannels towards the temperature change. As shown in **Figure 3a**, a prompt temperature change led to an instantaneous change of V_{oc}. To characterize the response speed quantitatively, we define the relative response speed, S, as,

$$S = \frac{t_T}{t_{V_{oc}}} \times 100\% \qquad (8)$$

where $t_{V_{oc}}$ is the time spent on the increase of V_{oc} from the initial value to the maximum. t_T is the time spent on the corresponding temperature change. From the data shown in **Figure 3a**, the value of S is 98.66 ± 0.02%, indicating the hybrid nanochannels have a very fast response to temperature change.

Another feature that can be found in **Figure 3a** is the stability and reproducibility of thermoelectric response to the temperature change. Upon recycling the temperature change, namely heating and cooling repetitively, the prompt variation of V_{oc} was maintained. The values of ΔV_{oc} recorded at a fixed ΔT (10 K) for seven cycles are compared in **Figure 3b**. Clearly, there is no significant loss or increase of ΔV_{oc} upon changing temperature, with an average value of 6.10 ± 0.14 mV for ΔV_{oc}.

In organisms, the temperature change is translated into a change of trans-nanochannel diffusion potential, namely $\Delta\phi_{diff}$, which is different from ΔV_{oc} measured in our experiment. As discussed in the theoretical section, ΔV_{oc} also includes the contribution of difference of redox potentials of two Ag/AgCl electrodes (namely ΔE_{redox}, see the details in the supporting information). $\Delta\phi_{diff}$ can be estimated by subtracting ΔE_{redox} from experimentally measured ΔV_{oc}, according to the equivalent circuit shown in **Figure 1b**. We determined ΔE_{redox} for different temperature change experimentally, which in fact are close to theoretical values (as

shown in **Figure S5**). **Figure 3c** displays the dependence of calculated $\Delta\phi_{diff}$ on ΔT and linear fitting to **eq. 4**. From the slope, t_+ was estimated to be 0.93, proving again an excellent cationic selectivity of SIM/PET hybrid nanochannels.

As proved above, the cationic selectivity of hybrid nanochannels is crucial to achieve a high sensitivity of thermosensation. In principle, when the solution temperature (e.g., $T_{b\text{-}SIM}$) increases, the variation of Gibbs free energy of solution (dG) follows the following equation

$$dG = -SdT + Vdp + \sum_{i=1} \mu_i \, d\, n_i \qquad (9)$$

where G, S, T, V and p are the Gibbs free energy, entropy, temperature, volume and pressure of solution. μ_i and n_i are the chemical potential and the molar number of species i. So a temperature change will drive the transport of ions in the opposite direction of temperature gradient. Meanwhile, the increase of temperature will cause the increase of diffusion coefficients of ions according to the Einstein-Stokes equation. In order to gain more insight on the thermally agitated ion transport, finite element simulations based on coupled Poisson-Nernst-Plank and Einstein-Stokes equations was carried out. The details on the simulation model and boundary conditions were given in the supporting information (see **Figure S6** and **Table S1**). First of all, from the calculated 2D concentration distribution of K^+ (see **Figure 4a**), we can clearly see the accumulation of K^+ inside SIM nanochannel and to the surface of nanochannel. It thus confirms the highly cationic selectivity of nanochannel, arising from the negatively charged surface of silica nanochannel and strongly overlapped electric double layer (EDL) in nanochannel.

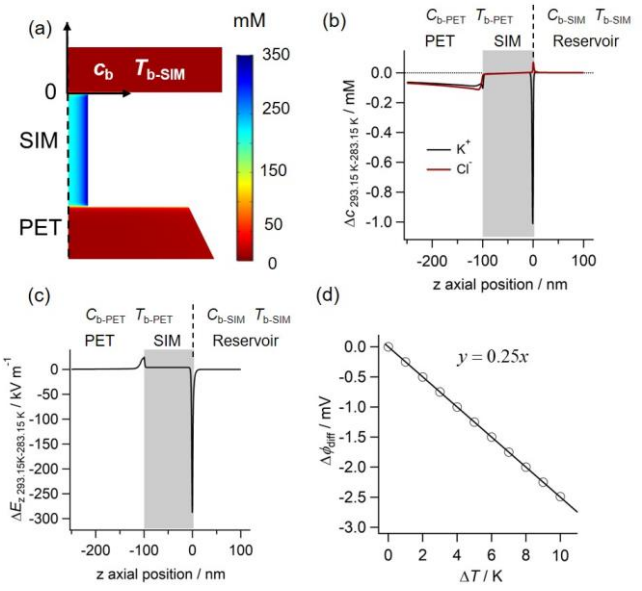

Figure 4. (a) Numerical simulation of the distribution of K^+ inside hybrid nanochannel. $T_{b\text{-}SIM}$ and c_b are set to 283.15 K and 10 mM, respectively. (b, c) The net variation of concentration (b) (Δc_z; K^+, black curve; Cl^-, red curve) and electric field (c) (ΔE_z, $E_z = -\partial\phi/\partial z$) along the axial direction of nanochannel for ΔT = 10 K ($\Delta T_{b\text{-}SIM}$ = 10 K, $T_{b\text{-}SIM}$ is varied from 283.15 K to 293.15 K; $T_{b\text{-}PET}$ = 283.15 K remains unchanged). The gray region (–100 nm ≤ z ≤ 0 nm) refers to SIM nanochannel, the region (–250 nm ≤ z ≤ –100 nm) denotes PET channel, and the region (0 nm ≤ z ≤ 100 nm) represents the reservoir solution, respectively. (d) Calculated $\Delta\phi_{diff}$ as a function of ΔT. The solid line represents the fitting by **eq. 4**.

To explore the origin of temperature-responsive electric signal, we plot the ionic concentration profile (c_z, for both K^+ and Cl^-) and electric field (E_z) along the axial direction of nanochannel before and after a temperature change of 10 K. The initial temperature of two solutions is set at 283. 15 K ($T_{b\text{-}SIM}$ = $T_{b\text{-}PET}$ = 283.15 K). $T_{b\text{-}SIM}$ is then increased by 10 K to 293.15 K, while $T_{b\text{-}PET}$ remains unchanged at 283.15 K. For simplicity, a sharp temperature boundary is assumed to exist at the SIM/reservoir solution interface (namely silica nanochannel orifice). The simulation results are shown in **Figures 4** and **S6**. Because it is hard to recognize directly the variations of c_z and E_z (see **Figure S7**), we here analyze the net variations, namely Δc_z and ΔE_z. As shown in **Figure 4b**, at the orifice of nanochannel there appear a remarkable depletion of K^+ and slight accumulation of Cl^-. This scenario can be ascribed to the temperature change and nanochannel permselectivity. According to **eq. 9**, the direction of ion transport is opposite to the temperature gradient. When $T_{b\text{-}SIM}$ is increased, both K^+ and Cl^- transport from the solution contacted with PET to that with SIM nanochannels. On the other hand, K^+ and Cl^- are initially accumulated and depleted, respectively, in SIM nanochannels (see **Figure 7a**, **b**), namely there exists a remarkable K^+ and Cl^- concentration gradient. For K^+, both temperature and concentration gradients drive the outflow of K^+, giving rise to a significant depletion at the orifice. However, as for Cl^-, its outflow driven by the temperature gradient is counteracted by the inflow promoted by the concentration gradient, leading to a slight accumulation at the orifice. The asymmetric distribution of K^+ and Cl^- at the orifice thus results in a very sharp negative overshoot of ΔE_z, as shown in **Figure 4c**, which predominantly contributes to the measured ΔV_{oc}.

While at the boundary of PET/SIM and inside nanochannel, both K^+ and Cl^- are slightly depleted (see more discussion in the supporting information). It proves that the overall direction of ion transport is opposite to the temperature gradient. Note that, for simplicity, in the simulation we only considered a sharp temperature boundary at the orifice of SIM nanochannel and do not take into account the heat conduction either. The SIM was also assumed to be thermally insulating. Moreover, a single pore model was used and pore-pore interaction was neglected.

We also calculated the dependence of $\Delta\phi_{diff}$ on ΔT, as shown in **Figure 4d**. A linear relationship is obtained, which coincides with the experimental trend. A larger ΔT yields a bigger $\Delta\phi_{diff}$. From the slope of linear fitting, t_+ is estimated to be 0.85. Although the value is slightly smaller than the experimental one, due to possibly aforementioned oversimplifications, it is sufficient to prove the permselectivity of hybrid nanochannels.

Bionic Thermoelectric Response with Concentration Gradient. A remarkable gel under the shark's skin enables it to locate prey-rich thermal fronts. This gel with a high salt concentration can translate the thermal information into electrical potential.[24] We further imitated this thermosensation process using SIM/PET hybrid nanochannels in the presence of electrolyte concentration gradient (0.5/0.01 M NaCl). Experimentally, the SIM side was put in contact with the concentrated solution (namely $c_{b\text{-}SIM}$ = 0.5 M NaCl), given a better permselectivity of silica

nanochannels than PET conical channels, while the PET side with the dilute one (namely $c_{b\text{-}PET}$ = 0.01 M NaCl). The temperature of either solutions was changed to compare the sensitivity of thermosensation. Note that in this case the cationic selectivity of SIM/PET nanochannel is still excellent, as the initial V_{oc} was measured to be 158.5 mV without any temperature gradient. According to **eqs. 6** and **7**, a better thermosensation sensitivity is expected when $T_{b\text{-}PET}$ is varied, which is 6.6 times larger than the opposite case (namely $T_{b\text{-}SIM}$ is varied). **Figure 5a** displays the thermoelectric response for the former case. Clearly, both ΔV_{oc} and ΔT synchronously vary with time. Moreover, both ΔV_{oc} and $\Delta\phi_{diff}$ exhibit a linear dependence on ΔT (see **Figure 5b**). The linear fitting yields t_+ = 0.93, proving the highly cationic permselectivity of hybrid nanochannels. On the other hand, a temperature change of 1 K leads to ΔV_{oc} by 0.7 mV and $\Delta\phi_{diff}$ by 0.3 mV, which is comparable to the biological thermometer. In addition, the response speed is also very fast, as shown in **Figure 5c**. The value of S calculated in terms of **eq. 8** is 98.87 ± 0.03%. **Figure 5c** also confirms the stability and reproducibility of thermoelectric response of hybrid nanochannels in this system.

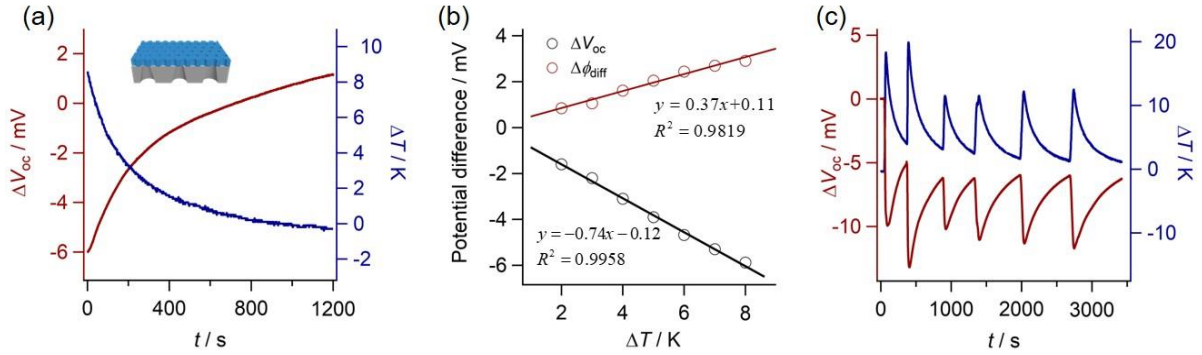

Figure 5. (a) Synchronous time evolution curves of ΔT ($\Delta T = |T_{b\text{-}SIM} - T_{b\text{-}PET}|$, blue curve) and ΔV_{oc} (red curve) of hybrid nanochannels in the presence of a concentration gradient. SIM and PET sides were put in contact with 0.5 M NaCl and 0.01 M NaCl, respectively. The temperature of dilute solution ($T_{b\text{-}PET}$) was varied. (b) ΔV_{oc} (black line) and $\Delta\phi_{diff}$ (red line) as a function of ΔT. The solid lines correspond to the linear fittings by **eqs. 6** and **7**, respectively. (c) ΔV_{oc} in response to ΔT for multiple cycles of temperature change.

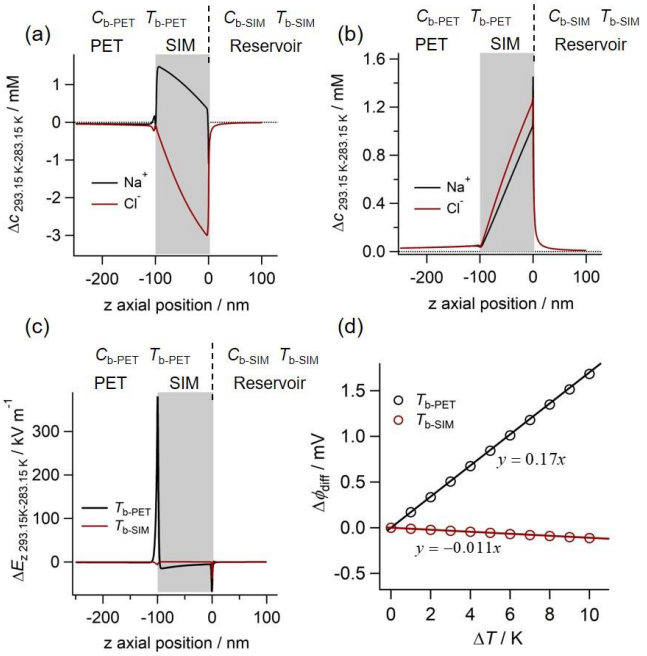

Figure 6. (a, b) The net variation of concentration of Na^+ (black curves) and Cl^- (red curves) along the axial direction of nanochannel in response to ΔT = 10 K in the dilute (a, $T_{b\text{-}PET}$ = 293.15 K, $T_{b\text{-}SIM}$ = 283.15 K) and concentrated solution (b, $T_{b\text{-}SIM}$ = 293.15 K, $T_{b\text{-}PET}$ = 283.15 K). (c) ΔE_z ($E = -\partial\phi/\partial z$) along the axial direction of nanochannel for ΔT = 10 K in the concentrated (black curve, $T_{b\text{-}PET}$ = 293.15 K, $T_{b\text{-}SIM}$ = 283.15 K) and dilute solution (red curve, $T_{b\text{-}SIM}$ = 293.15 K, $T_{b\text{-}PET}$ = 283.15 K). The gray region (–100 nm ≤ z ≤ 0 nm) refers to SIM nanochannel, the region (–250 nm ≤ z ≤ –100 nm) represents PET channel, and the region (0 nm ≤ z ≤ 100 nm) denotes the reservoir solution. (d) Calculated $\Delta\phi_{diff}$ as a function of ΔT ($\Delta T = |T_{b\text{-}SIM} - T_{b\text{-}PET}|$; $T_{b\text{-}PET}$ = 293.15 K, red line; $T_{b\text{-}SIM}$ = 293.15 K, black line): $c_{b\text{-}SIM}$ = 0.5 M, $c_{b\text{-}PET}$ = 0.01 M. The solid lines represent the fitting by **eq. 6**.

This bionic model with an electrolyte concentration gradient was also calculated by finite element simulations. The initial temperature of two solutions is set at 283. 15 K ($T_{b\text{-}SIM}$ = $T_{b\text{-}PET}$ = 283.15 K). Then either $T_{b\text{-}SIM}$ or $T_{b\text{-}PET}$ is increased to 293.15 K, and the other remains unchanged at 283.15 K. For simplicity, it is assumed that the sharp temperature boundary is located at the orifice of nanochannels in both cases (z = 0 in **Figure 6**). The concentration profiles of ions (for both Na^+ and Cl^-) at initial and final temperatures can be found in the supporting information (see **Figure S8a**, **b**). Here we first analyze Δc_z (for both Na^+ and Cl^-, see **Figure 6a**, **b**) and ΔE_z (see **Figure 6c**) along the axial direction of nanochannel in response to ΔT = 10 K. As shown in **Figure 6a**, after $T_{b\text{-}PET}$ is increased to 293.15 K, there appears depletion of both Na^+ and Cl^- at the orifice of nanochannel (z = 0). The depletion predominantly arises from the inflow of ions from SIM to PET side driven by the temperature difference in terms of **eq. 9**. While in the case of Na^+, its inflow is counteracted by a mild concentration gradient formed at the orifice due to nanochannel permselectivity (see the small upward overshoot in **Figure S8a**). As for Cl^-, the inflow is further enhanced by the concentration gradient (as shown in **Figure S8b**). That is why a more significant depletion of Cl^- than Na^+ is displayed at the orifice (z = 0), which results in a small negative overshoot of ΔE_z (as shown in **Figure 6c**). Inside nanochannel, there is an obvious accumulation of Na^+ and depletion of Cl^- in response to the temperature change, due to cationic selectivity of nanochannel. And the permselectivity turns better and better gradually toward the low concentration solution side. As we can see from **Figure S8a**, **b**, at the proximity of SIM/PET boundary the concentration of Na^+

is much higher than that of Cl^-. Therefore, a higher concentration gradient exists for Na^+, which results in a more significant concentration variation at the boundary. The asymmetric concentration of Na^+ and Cl^- gives rise to a very sharp positive overshoot of ΔE_z (as shown in **Figure 6c**), which predominately contributes to the observed ΔV_{oc}.

In the opposite case where $T_{b\text{-}SIM}$ is increased by 10 K to 293.15 K, the temperature gradient drives the outflow transport of both Na^+ and Cl^- from nanochannel to reservoir solutoin. However, as the neighboring reservoir solution contains a high concentration of ions, the concentration gradient resists the outflow, leading to their simultaneous accumulation at the orifice and thus a small negative overshoot of ΔE_z, as shown in **Figure 6b**. A smaller ΔE_z is indicative of a smaller $\Delta\phi_{diff}$, namely a lower thermosensation sensitivity in comparison with the former system. **Figure 6d** compares the calculated $\Delta\phi_{diff}$ as a function of ΔT for two cases. Indeed, the sensitivity of thermosensation is higher when the temperature of low concentration solution varies. This is in agreement with **eq. 7**, which predicts that the sensitivity is determined by the electrolyte concentration of solution where the temperature is changed.

CONCLUSIONS

In summary, a hybrid nanoporous membrane with a highly cationic selective nature was employed in this work as a bionic thermosensation platform. In response to the thermal stimulus, the permselective ion transport across hybrid nanochannels is translated into a trans-nanochannel potential difference, which can be recorded under the open-circuit condition as a measure of temperature change. Two bionic models, namely in the absence and presence of a concentration gradient, were studied to mimic the biological thermosensation processes by thermoTRP ion channels and shark, respectively. A thermal sensitivity of 0.7 mV/K was obtained, for two models, which is comparable to that of biological sensory system. Additionally, in both cases, the hybrid nanochannels display a rapid thermoelectric response to the thermal stimulus, with a relative response speed higher than 98%, as well as excellent stability and reversibility. Moreover, the experimental results coincide well with the theoretical relationship between electric signal and thermal stimulus derived in terms of a quasi-steady state ion transport model. The thermoelectric response was also rationalized to originate from temperature and concentration gradients by finite element simulations using coupled Poisson-Nernst-Plank and Einstein-Stokes equations. The thermal stimulus drives the ion transport along the direction of anti-temperature gradient, whereas the concentration gradient drives the ion transport in the same direction. The overall concentration gradient is determined by the bulk concentration of ions, but local concentration gradients exist in particular at the boundary of hybrid nanochannels due to their highly cationic selectivity. The permselectivity is a crucial parameter in the generation of a highly sensitive thermoelectric response. We believe this thermosensitive system can be further extended for mimicking ion channel based biosensation processes, for probing local temperature change of photothermal processes and for thermo-energy conversion.

EXPERIMENTAL SECTION

Materials and Reagents. All chemicals and reagents were used as received without further purification. All aqueous solutions were prepared with ultrapure water (18.2 MΩ cm). Tetraethoxysilane (TEOS, ≥99.0%), cetyltrimethylammonium bromide (CTAB, ≥98%), poly(methyl methacrylate) (PMMA, M_w = 996000) were purchased from Sigma-Aldrich. Potassium chloride (KCl, AR) and sodium chloride (NaCl, AR) were bought from Sinopharm Chemical Reagent. The aqueous solutions of KCl and NaCl were filtered with porous polyether sulfone membrane (pore size: 0.22 μm in diameter), prior to use.

ITO coated glass (surface resistivity <17 ohm/square, thickness 100 ± 20 nm) was ordered from Zhuhai Kaivo (Zhuhai, China). Prior to use, ITO was treated with 1 M NaOH solution, and then sonicated in acetone, ethanol, and deionized water sequentially. Ion-tracked PET membrane (12 μm in thickness; ion-track density: 10^8 cm^{-2}) was purchased from Wuwei Kejin Xinfa Co. Ltd.

Fabrication of Hybrid Nanochannels. The experimental details on the fabrication of SIM/PET hybrid nanochannels can be found in the supporting information (see **Figure S1**). Ion-track etched PET membrane consisting of conical nanochannels was prepared via the asymmetric etching.[19,25] The SIM consisting of highly ordered and perpendicular nanochannels was primarily growth on ITO glass by the Stöber-solution growth approach,[19] which was then exfoliated using the PMMA-assisted transfer technique reported recently.[20-22] The ion-track etched PET membrane was then employed to support SIM nanochannels with the tip surface of conical nanochannel PET membrane. The membrane area examined was 28.3 mm^2 (6 mm in diameter). Considering that the pore density of PET and SNM is ca. 10^8 cm^{-2} and 4×10^{12} cm^{-2}, and that the pore size of tip-side on PET and SNM is ca. 10 nm and 2.3 nm, respectively. The number of PET and SNM pores in this area was ca. 2.83×10^7 and 8.93×10^7, respectively.

Measurement and characterizations. Transmission electron microscopy (TEM, HT7700, Hitachi) and scanning electron microscopy (SEM, SU-8010 field-emission scanning electron microscope, Hitachi) were employed to characterize the morphology and structures of nanochannels. Ionic current measurement was carried out with Keithley 6847 picoammeter (Keithley Instruments, Cleveland). A pair of Ag/AgCl electrodes were used to supply voltage and measure the current.

The thermoelectric response was recorded by a custom-made setup. Briefly, a micro ceramic heater (Zhuhai Huiyou Electronics, China) was employed to regulate the temperature of one solution. A DC power (QJ6003S, Ningbo Jiuyuan Electronics, China) was connected to the heater to control the heating rate and temperature range. A pair of temperature microsensors (PT100, Tenghui Wenkong Instruments, China) were immersed in two solutions to measure the instantaneous temperature. The temperature and its change were real-time recorded and stored with a temperature sensor (THMA temperature

recorder, Tenghui Wenkong Instruments, China). The measurement accuracy and working range of the temperature sensor are ±0.15 K and -173.15 – 533.15 K, respectively. The trans-nanochannel potential was synchronously collected by an Autolab electrochemical workstation (PGSTAT302N, Metrohm) using two Ag/AgCl electrodes. The time resolutions of temperature recorder and trans-nanochannel potential are 1 s and 0.25 s, respectively.

Numerical simulation. Coupled Poisson-Nernst-Planck equation, continuum-based, was solved with by Comsol Multiphysics 5.2 package for a single hybrid nanochannel.[26] The hybrid nanochannel consists of a conical PET nanochannel connected with a SIM nanochannel. H^+ and OH^- are neglected, as their concentrations are much lower than that of majority ions (K^+, Na^+ or Cl^-). Furthermore, the surface charge density of PET, σ_{PET}, was considered as a constant (-0.002 C/m^2), and that of SIM was -0.015 C/m^2.[27] The details on the boundary conditions and simulation model were described in the supporting information.

ASSOCIATED CONTENT

Supporting Information. The experimental details on the preparation of hybrid nanochannels; the measurement of redox potential difference of Ag/AgCl electrodes; the theoretical derivation of open-circuit potential and trans-nanochannel potential; the details on finite element simulation model and boundary conditions. This material is available free of charge via the Internet at http://pubs.acs.org.

AUTHOR INFORMATION

Corresponding Author

*Prof. Bin Su, Email: subin@zju.edu.cn

All authors have given approval to the final version of the manuscript.

ORCID

Bin Su: http://orcid.org/0000-0003-0115-2279

Notes

The authors declare no competing financial interest.

ACKNOWLEDGMENT

This work was supported by the Natural Science Foundation of China (21575126 and 21874117) and the Zhejiang Provincial Natural Science Foundation (LZ18B050001).

REFERENCES

(1) Voets, T.; Talavera, K.; Owsianik, G.; Nilius, B. Sensing with TRP channels. Nat. Chem. Biol. 2005, 1, 85.

(2) de la Escosura-Muniz, A.; Merkoci, A. Nanochannels Preparation and Application in Biosensing. Acs Nano 2012, 6, 7556.

(3) Martin, C. R.; Siwy, Z. S. Learning Nature's Way: Biosensing with Synthetic Nanopores. Science 2007, 317, 331.

(4) Vriens, J.; Nilius, B.; Voets, T. Peripheral thermosensation in mammals. Nat. Rev. Neurosci. 2014, 15, 573.

(5) Delmas, P.; Hao, J.; Rodat-Despoix, L. Molecular mechanisms of mechanotransduction in mammalian sensory neurons. Nat. Rev. Neurosci. 2011, 12, 139.

(6) Voets, T. In Reviews of Physiology, Biochemistry and Pharmacology: Volume 162; Nilius, B., Amara, S. G., Gudermann, T., Jahn, R., Lill, R., Offermanns, S., Petersen, O. H., Eds.; Springer Berlin Heidelberg: Berlin, Heidelberg, 2012, p 91.

(7) Traversi, F.; Raillon, C.; Benameur, S. M.; Liu, K.; Khlybov, S.; Tosun, M.; Krasnozhon, D.; Kis, A.; Radenovic, A. Detecting the translocation of DNA through a nanopore using graphene nanoribbons. Nat. Nanotechnol. 2013, 8, 939.

(8) Huang, K.; Szleifer, I. Design of Multifunctional Nanogate in Response to Multiple External Stimuli Using Amphiphilic Diblock Copolymer. J. Am. Chem. Soc. 2017, 139, 6422.

(9) Zhang, D.; Zhou, S.; Liu, Y.; Fan, X.; Zhang, M.; Zhai, J.; Jiang, L. Self-Assembled Porphyrin Nanofiber Membrane-Decorated Alumina Channels for Enhanced Photoelectric Response. ACS Nano 2018, 12, 11169.

(10) Zhao, X.-P.; Wang, S.-S.; Younis, M. R.; Xia, X.-H.; Wang, C. Asymmetric Nanochannel–Ionchannel Hybrid for Ultrasensitive and Label-Free Detection of Copper Ions in Blood. Anal. Chem. 2017, 90, 896.

(11) Reber, N.; Küchel, A.; Spohr, R.; Wolf, A.; Yoshida, M. Transport properties of thermo-responsive ion track membranes. J. Membr. Sci. 2001, 193, 49.

(12) Jung, Y.; Bayley, H.; Movileanu, L. Temperature-Responsive Protein Pores. J. Am. Chem. Soc. 2006, 128, 15332.

(13) Yameen, B.; Ali, M.; Neumann, R.; Ensinger, W.; Knoll, W.; Azzaroni, O. Ionic Transport Through Single Solid-State Nanopores Controlled with Thermally Nanoactuated Macromolecular Gates. Small 2009, 5, 1287.

(14) Guo, W.; Xia, H. W.; Xia, F.; Hou, X.; Cao, L. X.; Wang, L.; Xue, J. M.; Zhang, G. Z.; Song, Y. L.; Zhu, D. B.; Wang, Y. G.; Jiang, L. Current Rectification in Temperature-Responsive Single Nanopores. Chemphyschem 2010, 11, 859.

(15) Zhang, Z.; Xie, G.; Xiao, K.; Kong, X.-Y.; Li, P.; Tian, Y.; Wen, L.; Jiang, L. Asymmetric Multifunctional Heterogeneous Membranes for pH- and Temperature-Cooperative Smart Ion Transport Modulation. Adv. Mater. 2016, 28, 9613.

(16) Zhou, Y.; Guo, W.; Cheng, J.; Liu, Y.; Li, J.; Jiang, L. High-Temperature Gating of Solid-State Nanopores with Thermo-Responsive Macromolecular Nanoactuators in Ionic Liquids. Adv. Mater. 2012, 24, 962.

(17) Hwang, J.; Sekimoto, T.; Hsu, W.-L.; Kataoka, S.; Endo, A.; Daiguji, H. Thermal dependence of nanofluidic energy conversion by reverse electrodialysis. Nanoscale 2017, 9, 12068.

(18) Taghipoor, M.; Bertsch, A.; Renaud, P. Temperature Sensitivity of Nanochannel Electrical Conductance. ACS Nano 2015, 9, 4563.

(19) Teng, Z.; Zheng, G.; Dou, Y.; Li, W.; Mou, C.-Y.; Zhang, X.; Asiri, A. M.; Zhao, D. Highly Ordered Mesoporous Silica Films with Perpendicular Mesochannels by a Simple Stöber-Solution Growth Approach. Angew. Chem., Int. Ed. 2012, 51, 2173.

(20) Lin, X.; Yang, Q.; Ding, L.; Su, B. Ultrathin Silica Membranes with Highly Ordered and Perpendicular Nanochannels for Precise and Fast Molecular Separation. ACS Nano 2015, 9, 11266.

(21) Wu, W.; Yang, Q.; Su, B. Centimeter-scale continuous silica isoporous membranes for molecular sieving. J. Membr. Sci. 2018, 558, 86.

(22) Zhao, M.; Wu, W.; Su, B. pH-Controlled Drug Release by Diffusion through Silica Nanochannel Membranes. ACS Appl. Mater. Interfaces 2018, 10, 33986.

(23) Wei, C.; Bard, A. J.; Feldberg, S. W. Current Rectification at Quartz Nanopipet Electrodes. Anal. Chem. 1997, 69, 4627.

(24) Brown, B. R. Sensing temperature without ion channels. Nature 2003, 421, 495.

(25) Apel, P. Y.; Korchev, Y. E.; Siwy, Z.; Spohr, R.; Yoshida, M. Diode-like single-ion track membrane prepared by electro-stopping. Nucl. Instrum. Methods Phys. Res., Sect. B 2001, 184, 337.

(26) White, H. S.; Bund, A. Ion Current Rectification at Nanopores in Glass Membranes. Langmuir 2008, 24, 2212.

(27) Yan, F.; Yao, L.; Chen, K.; Yang, Q.; Su, B. An ultrathin and highly porous silica nanochannel membrane: toward highly

efficient salinity energy conversion. J. Mater. Chem. A 2019, 7, 2385.

Table of Contents